Light-phase prednisone promotes glucose oxidation in heart through novel transactivation targets of cardiomyocyte-specific GR and KLF15

Authors: Fadoua El Abdellaoui Soussi[1#], Hima Bindu Durumutla[1#], Hannah Latimer[1], Ashok Daniel Prabakaran[1], Kevin McFarland[1], Karen Miz[1], Kevin Piczer[1], Cole Werbrich[1], Mukesh K Jain[2], Saptarsi M Haldar[3], Mattia Quattrocelli[1,*]

[#] These Authors contributed equally

Affiliations:

[1] Molecular Cardiovascular Biology, Heart Institute, Cincinnati Children's Hospital Medical Center and Dept. Pediatrics, University of Cincinnati College of Medicine, Cincinnati, OH, USA;

[2] Dept Cell Biology and Biochemistry, Brown University, Providence, RI, USA;

[3] Amgen Research, South San Francisco, CA, USA; Gladstone Institutes, San Francisco, CA, USA and Dept Medicine, Cardiology Division, UCSF, San Francisco, CA, USA

*** Corresponding Author:** Mattia Quattrocelli, PhD, Molecular Cardiovascular Biology, Heart Institute, Cincinnati Children's Hospital Medical Center, 240 Albert Sabin Way T4.676, Cincinnati, OH 45229.
Email: mattia.quattrocelli@cchmc.org, tel: +1-513-517-1221.

Keywords – Glucocorticoids, prednisone, chrono-pharmacology, glucose uptake, pyruvate oxidation, Adipor1, mitochondrial pyruvate carrier, glucocorticoid receptor, KLF15.

Data availability - RNA-seq and ChIP-seq datasets reported here will be available upon completion of the peer-review process.

Conflicts of interest – MQ is listed as co-inventor on a patent application related to intermittent glucocorticoid use filed by Northwestern University (PCT/US2019/068,618). All other authors declare they have no competing interests.

ABSTRACT

Circadian time of intake determines the cardioprotective outcome of glucocorticoids in normal and infarcted hearts. The cardiomyocyte-specific glucocorticoid receptor (GR) is genetically required to preserve normal heart function in the long-term. The GR co-factor KLF15 is a pleiotropic regulator of cardiac metabolism. However, the cardiomyocyte-autonomous metabolic targets of the GR-KLF15 concerted epigenetic action remain undefined. Here we report that circadian time of intake determines the activation of a transcriptional and functional glucose oxidation program in heart by the glucocorticoid prednisone with comparable magnitude between sexes. We overlayed transcriptomics, epigenomics and cardiomyocyte-specific inducible ablation of either GR or KLF15. Downstream of a light-phase prednisone stimulation in mice, we found that both factors are non-redundantly required in heart to transactivate the adiponectin receptor expression (*Adipor1)* and promote insulin-stimulated glucose uptake, as well as transactivate the mitochondrial pyruvate complex expression *(Mpc1/2)* and promote pyruvate oxidation. We then challenged this time-specific drug effect in obese diabetic *db/db* mice, where the heart shows insulin resistance and defective glucose oxidation. Opposite to dark-phase dosing, light-phase prednisone rescued glucose oxidation in *db/db* cardiomyocytes and diastolic function in *db/db* hearts towards control-like levels with sex-independent magnitude of effect. In summary, our study identifies novel cardiomyocyte-autonomous metabolic targets of the GR-KLF15 concerted program mediating the time-specific cardioprotective effects of glucocorticoids on cardiomyocyte glucose utilization.

INTRODUCTION

Metabolic stress harms the heart in chronic metabolic disorders like obesity and type-2 diabetes, featuring at least two key defects: insulin resistance and impaired glucose oxidation. Insulin resistance in glucose uptake is a key metabolic insult in the type-2 diabetic heart and correlates with metabolic inflexibility: loss of glucose oxidation with dominating lipid oxidation [1], a substrate imbalance that promotes diastolic dysfunction [2]. Moreover, accumulating ceramides in the diabetic heart promote their lipotoxic effect on both insulin sensitivity and glucose uptake [3]. Past works have addressed the losses in glucose oxidation and insulin sensitivity as single lines of action, but comprehensive strategies to tackle those metabolic lesions in diabetic cardiomyopathy are still missing. Despite the latest advancements in therapeutics like SGLT2 inhibitors and GLP1 agonists and/or lifestyle interventions, cardiovascular disease still accounts for ~40% of deaths in diabetic patients [4] and this number is only rising. Here we report a completely unanticipated role for the glucocorticoid receptor and its co-factor Krüppel-like factor 15 in regulating insulin-sensitive glucose uptake and glucose oxidation in heart, a key clinical need to rescue cardiovascular morbidity in these patients.

The glucocorticoid receptor (GR) is expressed in virtually all cell types and is a primal regulator of energy metabolism through glucocorticoid (GC)-induced activation [5]. The GR is important for normal heart function and contractility, as shown by cardiomyocyte-specific constitutive GR-KO mice [6, 7], but the GR role in heart metabolism remains unknown. The GR requirement for normal heart function conflicts with the notion that chronic daily intake of synthetic GCs promotes metabolic syndrome and heart failure [8]. We recently demonstrated that once-weekly intermittent intake of the GC prednisone reverts the metabolic stress and insulin resistance induced by once-daily intake of the same GC dose [9]. GC intermittence appears applicable and potentially effective in humans, as suggested by pilot clinical data of exercise tolerance obtained from adult dystrophic patients [10]. Notably for the context of heart failure, a once-weekly 1mg/kg prednisone treatment partially rescued cardiac function and bioenergetics after myocardial infarction in mice [11]. Moreover, the Krüppel-like factor 15 (KLF15) is a glucocorticoid-responsive GR target and co-factor [12]. Cardiomyocyte-specific KLF15 determines many nutrient utilization pathways in the heart, including lipids and branched chain amino acids [13, 14]. However, the cardiomyocyte-autonomous metabolic targets of the GR-KLF15 concerted epigenetic action remain undefined.

Regarding circadian time of GC intake, it must be noted that the GR regulates and is in turn regulated by core components of the circadian clock [15, 16]. Each day, the GR has a specific time window (early light-phase in mice) where it is highly responsive to exogenous GCs [17, 18] thanks to the overlay of endogenous corticosterone trough [19] with cyclical inhibitory actions by clock factors [17, 20]. Intriguingly, also the cardiomyocyte KLF15 appears mechanistically linked to circadian oscillations of the transcriptional and metabolic programs in heart [21]. Furthermore, we recently reported that circadian time of intake determines the cardioprotective GC action in normal and infarcted hearts. Specifically, a single prednisone pulse induced pro-energetic effects in the myocardium when dosed in the light-phase (ZT0, lights-on) but not in the dark-phase (ZT12, lights-off) [11]. However, the molecular mediators of GC chrono-pharmacology remain

unidentified.

Here we leverage our circadian-specific intermittent GC treatment to unveil unanticipated cardioprotective targets dependent on the non-redundant transactivation activity by the circadian-specific drug stimulation. We overlay epigenomics, transcriptomics and inducible cardiomyocyte-specific KO to find that the cardiomyocyte-specific GR and KLF15 are non-redundantly required for drug-induced insulin sensitization and glucose oxidation. We finally challenge the relevance of this pathway for cardiac functional rescue in obese diabetic mice. Our study challenges the current notions of glucocorticoid biology to identify novel druggable mechanisms of GR-KLF15 interplay to potentially help the heart overcome metabolic inflexibility during failure.

RESULTS

Light-phase dosing gates the glucocorticoid effects on cardiomyocyte glucose metabolism

In prior published work, we reported that circadian time-of-intake gated the cardioprotective effects of the glucocorticoid prednisone in infarcted murine hearts [11]. Through subsequent analysis of the RNA-seq datasets obtained from uninjured (sham-operated) myocardial tissues from that study (GSE186875), we found that compared to vehicle control ZT0 intermittent prednisone (once-weekly i.p. 1mg/kg) increased glucose

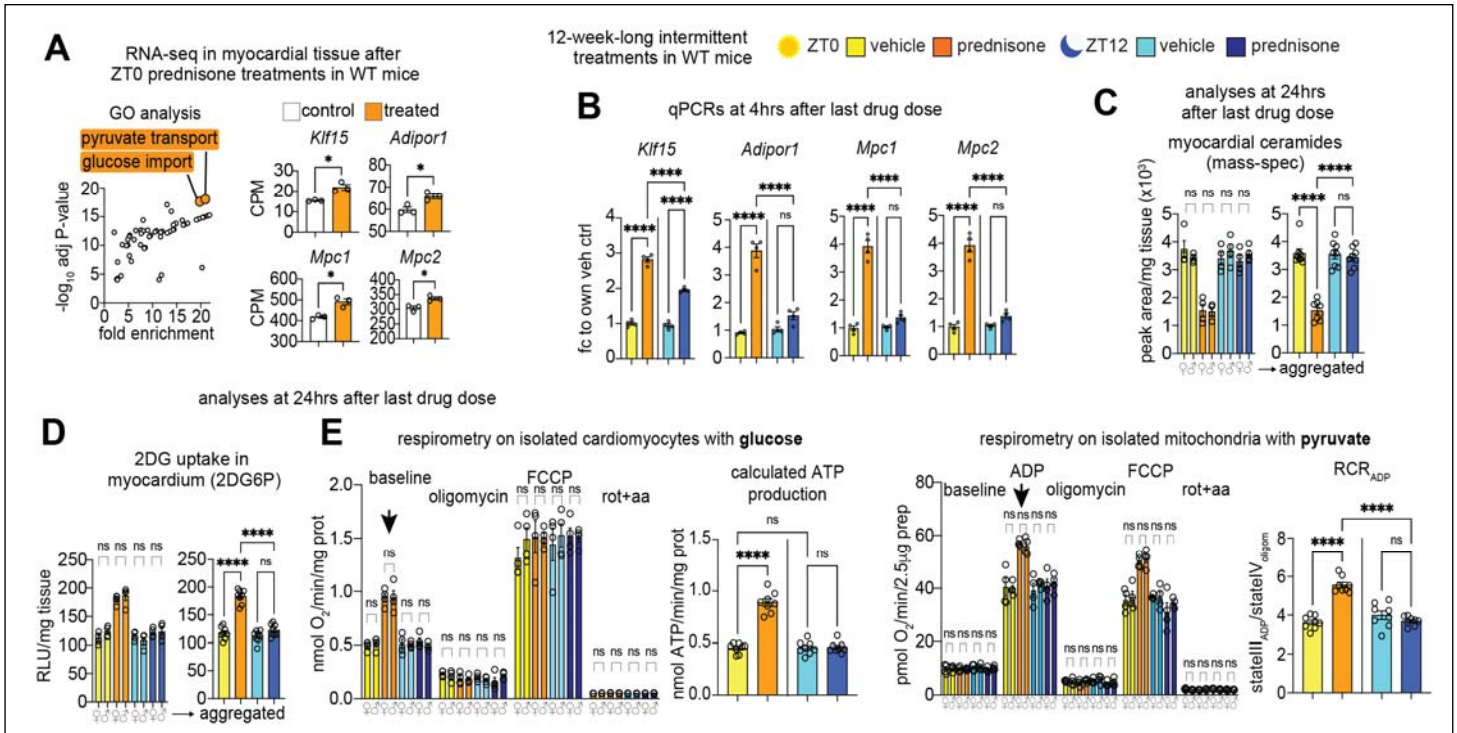

Figure 1. Light-phase glucocorticoid stimulation improves glucose uptake and oxidation in heart. (A) *Enrichment for GO terms related to glucose and pyruvate unveiled that ZT0 intermittent prednisone increased expression of Klf15, Adipor1, Mpc1 and Mpc2 in the WT heart.* ***(B)*** *These expression trends were specific to ZT0 drug stimulation, as they were blunted by ZT12 intake.* ***(C-D)*** *Consistent with Adipor1 upregulation, ZT0 prednisone treatment decreased myocardial ceramide abundance and increased insulin-dependent 2DG uptake in heart, independent from sex.* ***(E)*** *After ZT0 treatment, cardiomyocytes increased glucose-fueled respiration ex vivo (arrow), producing more ATP than control or ZT12 treatment. Consistent with Mpc1/2 upregulation ZT0 treatment increased ADP-stimulated respiration (arrow) and respiratory control ratio with pyruvate. These effects were sex independent. A: Welch's t-test; B-E: 2w ANOVA + Sidak; *, P<0.05; **, P<0.01; ***, P<0.001; ****, P<0.0001.*

import and pyruvate transport pathways. Among the genes encompassed in those two pathways, we found the remarkable upregulation of *Klf15*, *Adipor1* and *Mpc1/2* **(Fig. 1A)**. We found these gene trends remarkable: *AdipoR1* encodes the adiponectin-activated ceramidase that is sufficient to promote insulin-sensitive glucose uptake [22, 23]; *Mpc1/2* encode the two subunits of the mitochondrial pyruvate carrier, which is required for cardioprotective pyruvate oxidation [24-26]; *Klf15* encodes the homonymous epigenetic regulator of cardiac nutrient metabolism [13, 21, 27, 28], yet the specific targets of the KLF15 concerted program with its co-factor GR [12] remain unknown. Notably, these expression trends were specific or maximized by ZT0 vs ZT12 prednisone stimulation, as shown in validation qPCR experiments after 12-week-long treatments **(Fig. 1B)**. To monitor the extent to which these gene trends were significant for cardiac metabolic remodeling, we quantitated myocardial ceramide abundance through mass-spec in myocardial tissue, glucose uptake through 2-deoxyglucose (2DG) assay in vivo, and glucose oxidation through glucose-fueled respirometry in isolated cardiomyocytes and pyruvate-fueled respiratory control ratio (RCR) [29] in myocardial-derived isolated mitochondria, analyzing data as disaggregated and aggregated by sex. In line with *Adipor1* upregulation, ZT0 but not ZT12 prednisone decreased myocardial ceramides and increased insulin-dependent 2DG uptake in the heart, and the trends were sex-independent **(Fig. 1C-D)**. Moreover, ZT0 but not ZT12 prednisone treatment significantly increased the glucose-fueled respiration and calculated ATP production *in cardiomyocytes* **(Fig. 1E, left)**. Consistent with the upregulation of *Mpc1/2*, ZT0 but not ZT12 treatment also elevated ADP-stimulated respiration in mitochondria, increasing pyruvate-fueled RCR **(Fig. 1E, right)**. The effects in cardiomyocytes and mitochondria were sex-independent. Therefore, light-phase (ZT0, lights-on) dosing unveiled a functionally relevant glucocorticoid-stimulated gene program concertedly linking glucose uptake to oxidation in the uninjured WT heart.

Light-phase prednisone promotes a concerted epigenetic program of GR and KLF15 in heart

Considering the *Klf15* upregulation and the expected GR activation, we sought to test the extent to which the GR-KLF15 axis mediated the upregulation of *AdipoR1* and *Mpc1/2* upregulation by light-phase glucocorticoids through a direct cardiomyocyte-autonomous effect. Considering novelty and potential significance of those targets for both GR and KLF15 in heart, we decided to employ the unbiased rigorous strategy of overlaying ChIP-seq for the two factors with RNA-seq datasets comparing cardiomyocyte-specific inducible KO versus WT for each factor. To profile their epigenomic occupancy in myocardial tissue, we performed parallel GR and KLF15 ChIP-seq in myocardial tissue at 4-hours after a single pulse of light-phase prednisone, adapting the method we previously reported for muscle [30]. Because no ChIP-seq-grade commercial antibodies are available for KLF15, we performed the immunoprecipitations in myocardial tissue of KLF15-3xFLAG$^{+/-}$ knock-in mice [31]. To profile the myocardial transcriptome in presence versus absence of each factor, we used mice with cardiomyocyte-specific inducible ablation of each factor. For the GR, we used the transgenic mice we already reported [11], comparing *Myh6-MerCreMer*$^{+/-}$*;Nr3c1*$^{fl/fl}$ (GR-KO) and *Myh6-MerCreMer*$^{+/-}$

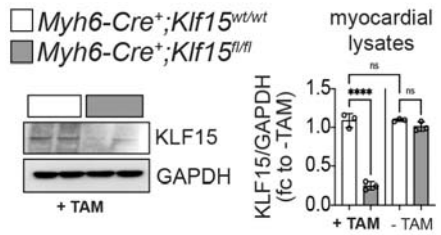

Figure 2. Validation of inducible KLF15 ablation in heart. *Compared to Cre^{+};Klf15$^{wt/wt}$ and non-tamoxifen controls, KLF15 was ~85% ablated by tamoxifen in Cre^{+}/Klf15$^{fl/fl}$ hearts. 2w ANOVA + Sidak; *, P<0.05; **, P<0.01; ***, P<0.001; ****, P<0.0001.*

;Nr3c1$^{wt/wt}$ (GR-WT) hearts immediately after the tamoxifen-induced ablation and washout protocol. Analogously, we generated cardiomyocyte-specific inducible KLF15-KO mice by crossing the *Myh6-MerCreMer* with the *Klf15-floxed* allele [21]. We verified tamoxifen-induced Klf15 ablation in the postnatal heart (Fig. 2), using the same tamoxifen and washout protocol used for the GR-KO mice. Also for KLF15, we compared *Myh6-MerCreMer$^{+/-}$;Klf15$^{fl/fl}$* (GR-KO) and *Myh6-MerCreMer$^{+/-}$;Klf15$^{wt/wt}$* (GR-WT) hearts. For both ChIP-seq and RNA-seq dataset generation, we collected the myocardial tissues at 4 hours after a single ZT0 prednisone injection, to analyze epigenomic-transcriptomic changes in the absence of long-term secondary effects.

Regarding the ChIP-seq datasets, unbiased motif analysis revealed high enrichment for each factor's canonical binding motif, validating the specificity of GR and KLF15 immunoprecipitations **(Fig. 3A)**. Both GR and KLF15 appeared activated in their epigenomic activity by the ZT0 prednisone pulse, as shown by increased peak number and increased signal over canonical sites genome-wide, albeit no drug-driven changes were noted in the peak localization that was highly enriched in promoter-transcriptional start sites (TSS) **(Fig. 3B)**. Regarding the gene ablation effects on transcriptional profiles, principal component analysis (PCA) of the RNA-seq datasets clustered

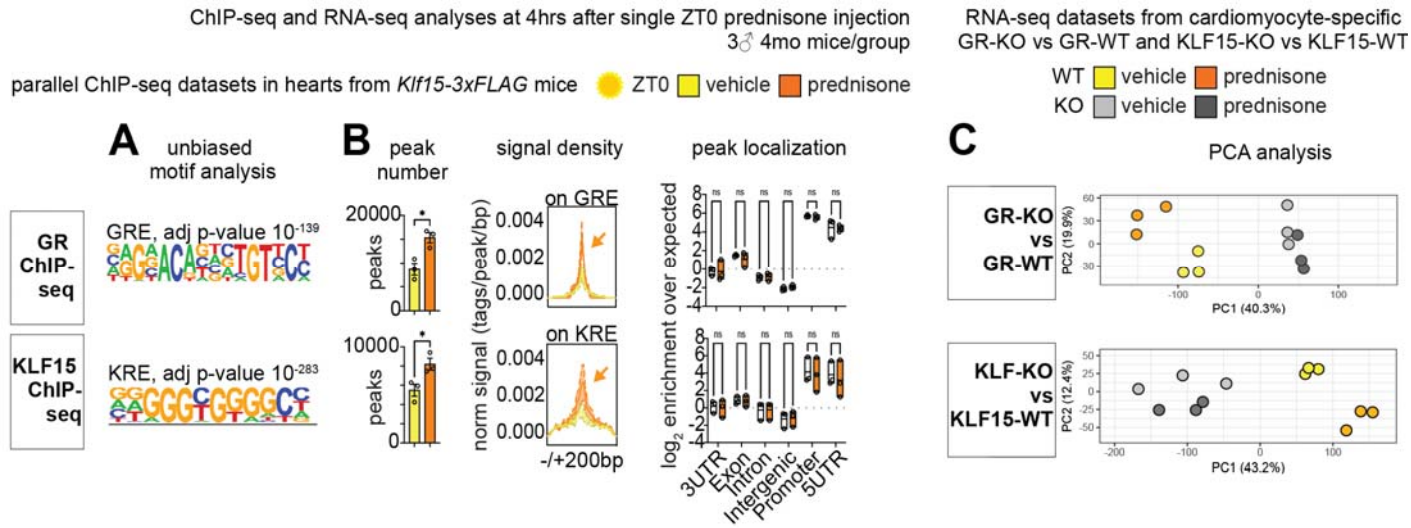

Figure 3. ChIP-seq and RNA-seq datasets reveal non-redundant mediator effect of both cardiomyocyte-specific GR and KLF15 on ZT0 glucocorticoid gene programs in heart. (A) *Validation of ChIP-seq datasets through unbiased motif analysis.* ***(B)*** *Prednisone increased peak numbers and canonical epigenomic peak signal (arrows) for both GR and KLF15 without changes in relative enrichment in genomic localization, which was prevalent in promoter and 5'UTRs for both factors.* ***(C)*** *PCA analyses show sample clustering according to drug and genotype variables. B: peak number, Welch's t-test; peak localization, 2w ANOVA + Sidak; *, P<0.05; **, P<0.01; ***, P<0.001; ****, P<0.0001.*

samples according to drug and cardiomyocyte genotype for either GR or KLF15 **(Fig. 3C)**. Thus, we generated unbiased genome-wide datasets that reveal a concerted epigenetic activation and a cardiomyocyte-autonomous role in the transcriptional response to light-phase glucocorticoids for GR and KLF15.

Cardiomyocyte GR and KLF15 are independently required to transactivate Adipor1, promoting ceramide reduction and insulin-driven glucose uptake.

We first tested the extent to which *AdipoR1* was a direct transactivation target of GR and KLF15 in heart downstream of ZT0 prednisone. ChIP-seq tracks revealed steroid-sensitive peaks on the *Adipor1* proximal promoter for both GR and KLF15. RNA-seq analysis revealed that the inducible cardiomyocyte-specific ablation of either GR or KLF15 blunted the drug-induced upregulation of *Adipor1*, demonstrating the non-redundant requirement of both transcription factors for ZT0 prednisone transactivation of *Adipor1* in heart **(Fig. 4A)**. Furthermore, we tested the extent to which the *AdipoR1* expression regulation by GR and KLF15 was impactful on ceramide and glucose uptake comparing KO versus WT hearts after 12-week-long treatments. Cardiomyocyte ablation of either GR or KLF15 blocked the long-term ZT0 prednisone effects on ceramide reduction and 2DG uptake in heart **(Fig. 4B)**. These data illustrate that both GR and KLF15 are required for the cardiomyocyte-

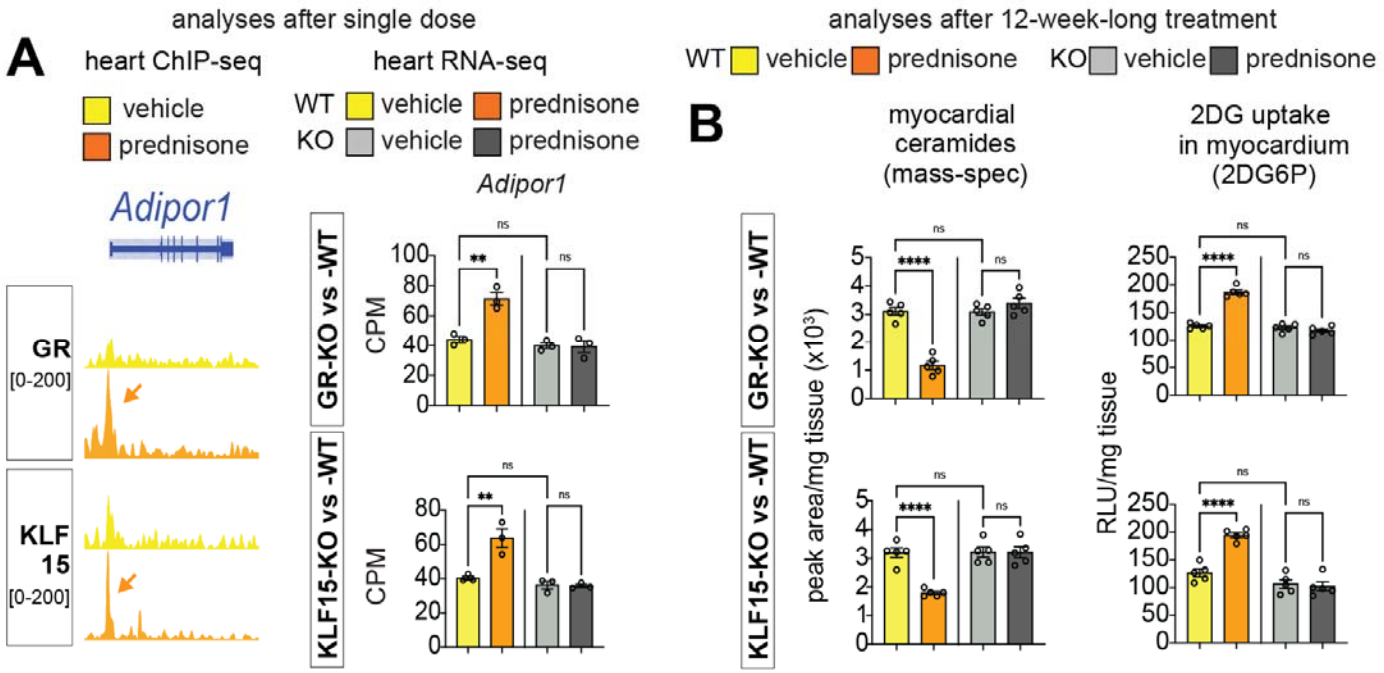

Figure 4. Cardiomyocyte GR and KLF15 are required for the ZT0 prednisone effects on Adipor1 transactivation, ceramide reduction and insulin sensitization in heart. (A) *GR and KLF15 showed steroid-sensitive peaks on Adipor1 TSS (arrows). Drug-induced upregulation was blunted by inducible cardiomyocyte-specific ablation of either GR or KLF15, demonstrating their non-redundant requirement for the ZT0 prednisone transactivation effect in heart.* ***(B)*** *Consistent with Adipor1 expression trends, GR and KLF15 were both required for the prednisone treatment effects on myocardial ceramide content reduction and insulin-stimulated glucose uptake increment in heart. 2w ANOVA + Sidak; *, P<0.05; **, P<0.01; ***, P<0.001; ****, P<0.0001.*

autonomous effects of ZT0 prednisone on *Adipor1* upregulation, ceramide depletion and insulin sensitization.

Cardiomyocyte GR and KLF15 are independently required to transactivate Mpc1/2, promoting pyruvate oxidation in heart.

We then tested the extent to which *Mpc1/2* were direct transactivation targets of cardiomyocyte-specific GR and KLF15 downstream of ZT0 prednisone. ChIP-seq tracks revealed steroid-sensitive peaks on the proximal promoters of *Mpc1* and *Mpc2* for both GR and KLF15. RNA-seq analysis revealed that the inducible cardiomyocyte-specific ablation of either GR or KLF15 blunted the drug-induced upregulation of both genes, demonstrating the non-redundant requirement of both transcription factors for ZT0 prednisone transactivation of *Mpc1/2* in heart **(Fig. 5A)**. Furthermore, we tested the extent to which the *Mpc1/2* expression regulation by GR and KLF15 was impactful on pyruvate oxidation comparing KO versus WT heart-derived mitochondria after 12-week-long treatments. Cardiomyocyte ablation of either GR or KLF15 blocked the long-term ZT0 prednisone

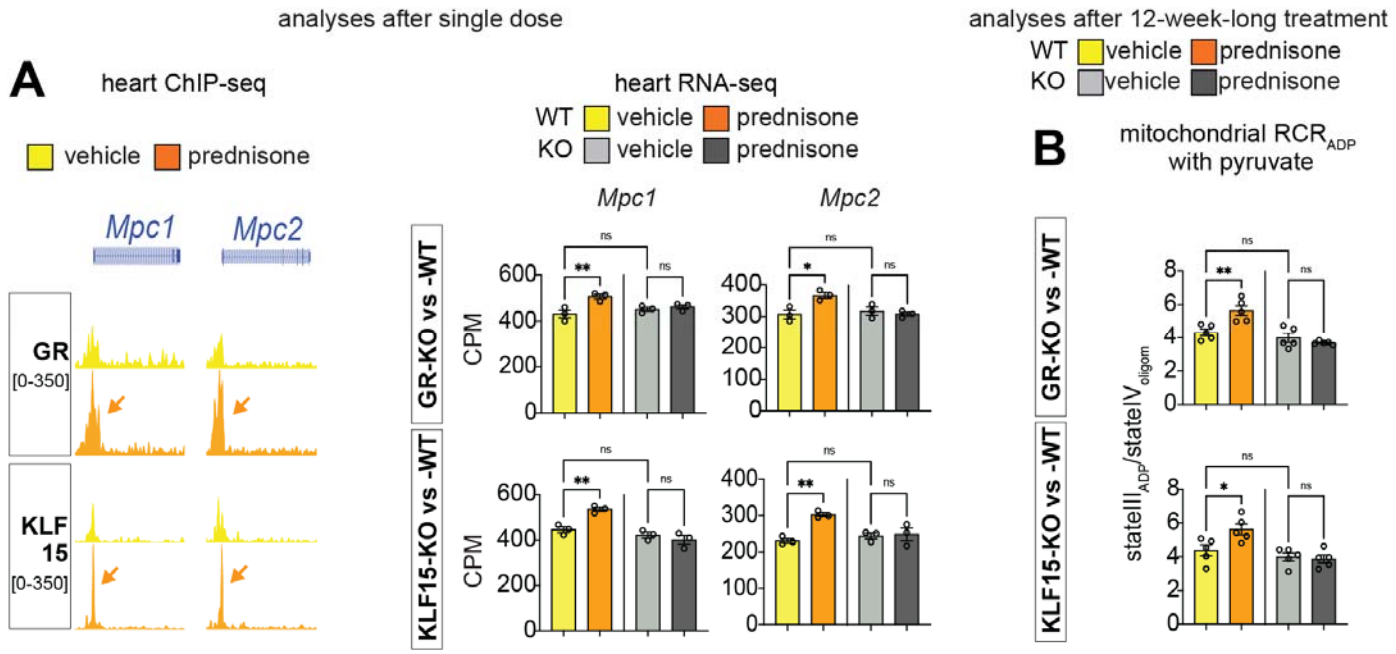

Figure 4. Cardiomyocyte GR and KLF15 are required for the ZT0 prednisone effects on Mpc1/2 transactivation and pyruvate oxidation in heart. (A) *GR and KLF15 showed steroid-sensitive peaks on Mpc1/2 TSS (arrows). Drug-induced upregulation was blunted by inducible cardiomyocyte-specific ablation of either GR or KLF15, demonstrating their non-redundant requirement for the ZT0 prednisone transactivation effect in heart.* ***(B)*** *Consistent with Mpc1/2 expression trends, GR and KLF15 were both required for the prednisone treatment effects on pyruvate-fueled respiration in heart-derived mitochondria. 2w ANOVA + Sidak; *, P<0.05; **, P<0.01; ***, P<0.001; ****, P<0.0001.*

effects on pyruvate-fueled mitochondrial RCR **(Fig. 5B)**. These data illustrate that both GR and KLF15 are required for the cardiomyocyte-autonomous effects of ZT0 prednisone on *Mpc1/2* upregulation and myocardial pyruvate utilization.

Light-phase glucocorticoid intermittence rescues glucose oxidation and diastolic function in db/db hearts.

We reasoned that the combination of insulin sensitization and pyruvate oxidation of light-phase glucocorticoid intermittence could be relevant as a "two-hit" strategy to promote a functional glucose oxidation program in heart. Considering that insulin resistance and impaired glucose oxidation are among the defining metabolic insults for type-2 diabetic cardiomyopathy [1, 2], we sought to challenge the relevance for this ZT0 prednisone program in a model of diabetic cardiomyopathy that recapitulates insulin resistance and diastolic dysfunction, 6mo *db/db* obese diabetic mice [32, 33].

We treated *db/db* mice (obese diabetic) and their *db/+* littermate lean controls at ~6 months of age for 12 weeks with ZT0 versus ZT12 intermittent prednisone. Compared to isochronic vehicle, ZT0 but not ZT12 treatment increased glucose-fueled basal respiration and ATP production in isolated cardiomyocytes, rescuing *db/db* levels to control-like levels without discernable sex-specific differences **(Fig. 6A)**. In vivo, treatment rescued diastolic dysfunction measured as E/e' ratio through Doppler echocardiography in *db/db* hearts towards control-like levels, aslwo without appreciable sexual dimorphism in the magnitude of effect **(Fig. 6B)**. Thus, the glucose oxidation program enabled by time-specific prednisone intermittence is functionally relevant in <u>*db/db*</u> cardiomyocytes and hearts.

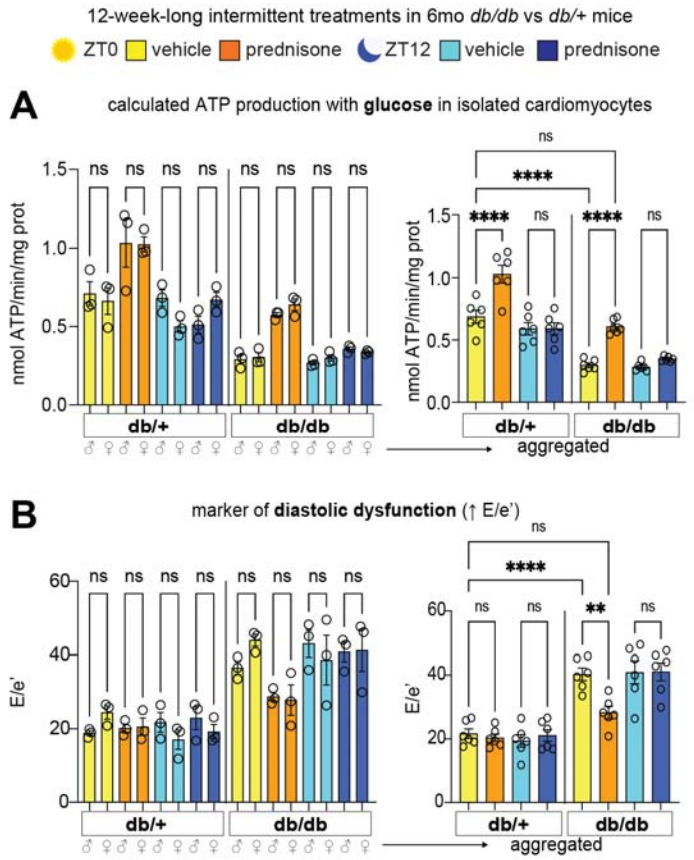

Figure 6. ZT0 glucocorticoid treatment rescues glucose oxidation and diastolic function in db/db mice. (A) *Treatment increased glucose-fueled ATP production calculated from Seahorse curves in isolated cardiomyocytes in both db/+ and db/db mice according to time of intake (ZT0), increasing db/db values to control-like levels.* ***(B)*** *Although no treatment effects were quantitated on E/e' values in db/+ controls, ZT0 prednisone decreased diastolic dysfunction to control-like levels, while the ZT12 treatment did not induce significant shifts. 3w ANOVA + Sidak; *, P<0.05; **, P<0.01; ***, P<0.001; ****, P<0.0001.*

DISCUSSION

The GR is a potent metabolic regulator that acts as transcription factor when activated by glucocorticoids. The cardiomyocyte-specific GR is important for heart function[7], but the cardiomyocyte-autonomous role of GR in heart metabolism remains unknown. Notably for this project, the GC-GR axis is tightly linked to the circadian rhythm [16] and to chronic dosing

frequency. Recently, we have shown two interconnected time dimensions that resolve benefits from detriments of GC pharmacology: 1) circadian time-of-intake: in mice, light-phase dosing of the GC prednisone improved function in WT and infarcted hearts, in contrast to dark-phase dosing [11]; 2) chronic frequency-of-intake: intermittent once-weekly prednisone dosing reversed the dysmetabolic effects of chronic daily dosing and improved exercise tolerance [9]. Remarkably, a pilot clinical trial with circadian-restricted intermittent prednisone in dystrophic patients improved lean mass and exercise tolerance [10], supporting feasibility and relevance for humans. GR activity is regulated by the circadian clock [17, 20], yet the specific targets of glucocorticoid chronopharmacology for functional cardiac metabolic remodeling remain poorly elucidated. Our data presented here unravel one such mechanism: the required epigenetic role for the GR-KLF15 axis in promoting the light-phase-specific glucocorticoid transactivation of *Adipor1* and the MPC complex in heart.

AdipoR1 is the adiponectin-responsive ceramidase enzyme [34] that, by degrading ceramides, directly promotes insulin-sensitive glucose uptake [35]. Indeed, AdipoR1 is the main ceramidase genetically linked to the pro-metabolic effects of adiponectin on insulin sensitivity [23]. Ceramides accumulate in heart with obesity and/or type-2 diabetes, promoting cardiac insulin resistance and the related cardiac dysfunction [36]. A pharmacological upregulation of AdipoR1 is notable not only for its direct ceramidase potential, but also for the emerging concept that an overt re-activation of glucose uptake could actually be counterproductive if not balanced by complementary remodeling, as shown by cardiomyocyte GLUT4 overexpression in hearts from diabetic mice [37]. In that perspective, our findings with the simultaneous upregulation of both AdipoR1 and the MPC complex could offer a model to reactivate both glucose uptake and downstream oxidation in a balanced fashion.

MPC expression is downregulated in failing human hearts [38] and transcriptional MPC abundance directly promotes cardioprotective oxidation of pyruvate and its precursor glucose in the myocardium [24, 25, 38]. Accordingly, MPC activity is decreased in the diabetic heart too [39]. It was remarkable to observe a strong concerted epigenetic program by the cardiomyocyte-specific GR and KLF15 on both subunit genes for the MPC, which indeed resulted in pyruvate oxidation trends in line with increased glucose oxidation.

In diabetic patients, endogenous glucocorticoids are elevated, likely as a response to metabolic stress . Indeed, compared to WT controls, obese diabetic mice show higher levels of corticosterone but still maintain diurnal rhythmicity, albeit dampened [40]. Intriguingly, despite these endogenous glucocorticoid changes, *db/db* mice appeared still susceptible to chrono-pharmacology with prednisone intermittence, particularly on its effects on glucose utilization and rescue of diastolic dysfunction. The question is still open on the extent to which this susceptibility to chrono-pharmacology is translatable to type-2 diabetic patients, although the pilot clinical data from adult dystrophic patients with lean mass and exercise tolerance are encouraging [10].

Limitations of the study – Despite the mechanistic evidence offered by cardiomyocyte-specific GR and KLF15 inducible ablation in non-diabetic conditions, in this study we did not cross-validate the requirement for both factors on the ZT0 prednisone effects in the db/db background. We believe this is beyond the scope of this investigation, and ablation of those pleiotropic factors in an already metabolically impaired cardiomyocytes could shift the overall balance towards non-physiologically relevant confounding effects.

Conclusions and overall impact – In summary, our study challenges the current paradigm of glucocorticoid cardiotoxicity by identifying a specific mechanism that mediates the circadian-gated glucocorticoid benefit on cardiomyocyte glucose oxidation, with functional implications for diabetic cardiomyopathy.

Acknowledgements - Mass-spec analyses were performed thanks to the Mass-Spec Metabolomics Core Facility at Robert H. Lurie Comprehensive Cancer Center of Northwestern University, with critical assistance by Dr. Gao. Next-gen sequencing was performed thanks to the Cincinnati Children's DNA Sequencing and Genotyping Facility (RRID: SCR_022630), with critical assistance by David Fletcher, Keely Icardi, Julia Flynn, and Taliesin Lenhart.

Grant support – This work was supported by R56HL158531-01, R01HL166356-01, R03DK130908-01A1, R01AG078174-01 (NIH) and RIP, CCRF Endowed Scholarship, HI Translational Funds (CCHMC) grants to MQ.

MATERIAL AND METHODS

Animal handling and treatments

Mice were housed in a pathogen-free facility in accordance with the American Veterinary Medical Association (AVMA) and under protocols fully approved by the Institutional Animal Care and Use Committee (IACUC) at the Cincinnati Children's Hospital Medical Center (#2023-0002). Consistent with the ethical approvals, all efforts were made to minimize suffering. Euthanasia was performed through carbon dioxide inhalation followed by cervical dislocation and heart removal.

Mice were maintained on a 12h/12h light/dark cycle, and diet/pharmacological treatments were initiated at ~ 12 weeks of age. Mice were obtained and interbred from the Jakson Laboratories (Bar Harbor, ME; JAX strain number listed) or from collaborators: WT C57BL/6 mice #000664, Myh6-MerCreMer mice #005657, GR-flox mice #021021, Klf15-flox mice #029787 (provided by Dr. Jain, Brown U), db/db #000642; KLF15-3xFLAG mice [31] were provided by Dr. Haldar (Amgen & UCSF). Gene ablation was induced with tamoxifen at ~8 weeks of age using a combination of i.p. (20 mg/kg/day for 5 days; Sigma #T5648) and chow-mediated (40mg/kg for 3 weeks; Harlan #TD.130,860) administration. Analyses were performed after 4 weeks of tamoxifen washout, i.e. at ~16 weeks of age. Weekly prednisone treatment consisted of once-weekly intraperitoneal injection of prednisone (1 mg/kg; #P6254, Sigma-Aldrich, St. Louis, MO). The injectable solution was diluted from a stock (5 mg/ml) in dimethyl sulfoxide (DMSO; #D2650, Sigma-Aldrich, St. Louis, MO) in a 50-µl volume. Injections

were conducted either at the beginning of the light phase (ZT0; lights on) or at the beginning of the dark phase (ZT12; lights off). Tissues were harvested at 4 hours post-injection for epigenetic/transcriptional assays and at 24 hours post-injection for metabolic/physiologic assays. All in vivo, ex vivo, and postmortem analyses were conducted blinded to treatment group.

RNA-seq and qPCR analyses

RNA-seq was conducted on RNA extracted from left ventricle myocardial tissue. Each heart was immediately snap frozen in 1ml TRIsure (Bioline, BIO-38033) using liquid nitrogen. RNAs from each heart were re-purified using RNeasy Mini Kit (Cat #74104; Qiagen, Germantown, MD). RNA-seq was performed at the DNA Core (CCHMC). 150 ng – 300 ng of total RNA determined by Qubit (Cat #Q33238; Invitrogen, Waltham, MA) high-sensitivity spectrofluorometric measurement was poly-A selected and reverse transcribed using Illumina's TruSeq stranded mRNA library preparation kit (Cat# 20020595; Illumina, San Diego, CA). Each sample was fitted with one of 96 adapters containing a different 8 base molecular barcode for high level multiplexing. After 15 cycles of PCR amplification, completed libraries were sequenced on an Illumina NovaSeqTM 6000, generating 20 million or more high quality 100 base long paired end reads per sample. A quality control check on the fastq files was performed using FastQC. Upon passing basic quality metrics, the reads were trimmed to remove adapters and low-quality reads using default parameters in Trimmomatic [Version 0.33]. In the next step, transcript/gene abundance was determined using kallisto [Version 0.43.1]. The trimmed reads were then mapped to mm10 reference genome using default parameters with strandness (R for single-end and RF for paired-end) option in Hisat2 [Version 2.0.5]. In the next step, transcript/gene abundance was determined using kallisto [Version 0.43.1]. We first created a transcriptome index in kallisto using Ensembl cDNA sequences for the reference genome. This index was then used to quantify transcript abundance in raw counts and counts per million (CPM). Differential expression (DE genes, FDR<0.05) was quantitated through DESeq2. PCA was conducted using ClustVis. Gene ontology pathway enrichment was conducted using the Gene Ontology analysis tool.

Total RNA was extracted from cryo-pulverized liver tissue and hiPSC-derived hepatocyte-like cells using Trizol (Thermo Fisher Scientific) and 1 ug RNA was reverse-transcribed using SuperScript^{TM} IV VILO^{TM} Master Mix (#11756050, Thermo Fisher Scientific). RT-qPCRs were conducted in three replicates using 1X SYBR Green Fast qPCR machine (Bio-Rad, Hercules, CA; thermal profile: 95C, 15 sec; 60C, 30sec; 40x; melting curve). The 2-$\Delta\Delta$CT method was used to calculate relative gene expression. GAPDH was used as the internal control. Primers were selected among validated primer sets from MGH PrimerBank as follows:

Gene	**Forward**	**Reverse**
Klf15	GAGACCTTCTCGTCACCGAAA	GCTGGAGACATCGCTGTCAT
Adipor1	TCTTCGGGATGTTCTTCCTGG	TTTGGAAAAAGTCCGAGAGACC
Mpc1	CTCCAGAGATTATCAGTGGGCG	GAGCTACTTCGTTTGTTACATGGC

Mpc2	CTCAGTCCACTGTGTTGATGGC	ATCCGAAACAGCTGAGAGGCTC

Mass-spec analysis of ceramides in myocardial tissue

Untargeted lipidomics was performed on myocardial tissue from mice treated for 12-week-long intermittent treatments with vehicle or weekly prednisone. Whole hearts were snap-frozen and then ground to powder with dry ice-chilled mortar and pestle. Frozen samples were sent on dry ice to mass spectrometry Core at the Cincinnati Children's Hospital Medical Center, where LC-MS and data analysis were performed. Briefly 10 µl sample was added to 30 µl of internal standard, except for the blank calibrator. Then 300 µl of Butanol/Methanol (3:1) was added to sample aliquot tube and vortexed for 10 mins. Next, 150 µl of Heptane/Ethyl Acetate (3:1) was added to the sample tube and vortexed for 5 mins. The contents of the sample aliquot were then transferred to a large glass tube, to which 150 µl of Heptane/Ethyle Acetate was added and vortexed for 5 mins. Then, 300 ul of 1% Acetic acid was added to the original tube to wash, vortexed for 5 mins and then added back to the glass tube. The glass tube was further vortexed for 5 mins and let sit for 5 mins. The upper organic phase of ~ 200 µl was transferred to a new glass tube. To this, 320 µl Heptane/Ethyl Acetate (3:1) was added to the water phase, vortexed for 5 mins and let sit for 5 mins. Next, 280 µl of upper organic phase (second extract) was transferred to the first extract. This step is repeated once. The upper organic phase (third extract) of 100 µl was combined with other extracts and dried down with nitrogen in a heating block set to 40°C. The resuspended lipid extracts (2 µl) were loaded and separated through Xevo QTOF G2-S mass spectrometer (Waters Corp). All calculations were performed using QuanLynx.

Chromatin immunoprecipitation sequencing

Whole hearts were cryopowdered using a liquid nitrogen-cooled RETSCH Cryomill. The cryopowdered tissue was then fixed in 10 ml of 1% paraformaldehyde (PFA) for 30 min at room temperature with gentle nutation. Fixation was quenched 1 ml of 1.375 M glycine (Cat# BP381-5, Thermo Fisher Scientific, Waltham, MA) with gentle nutation for 5 mins at room temperature. After centrifugation at 3,000*g* for 5 mins at 4°C, the pellet was resuspended in cell lysis buffer as per reported conditions, supplementing the cell lysis buffer with cytochalasin B (3 µg/ml) and rotating for 10 min at 4°C. Nuclei were pelleted at 300*g* for 10 mins at 4°C and subsequently processed following the reported protocol with the adjustment of adding cytochalasin B (3 µg/ml) into all solutions for chromatin preparation and sonication, antibody incubation, and wash steps. Chromatin was then sonicated for 15 cycles (30 s, high powder, 30-s pause, and 500-µl volume) in a water bath sonicator set at 4°C (Bioruptor 300. Diagenode, Denville, NJ). After centrifuging at 10,000*g* for 10 mins at 4°C, sheared chromatin was checked on agarose gel for a shear band comprised between ~150 and ~600 bp. Two micrograms of chromatin were kept for pooled input controls, whereas ~50 µg of chromatin was used for each pull-down reaction in a final volume of 2 ml rotating at 4°C overnight. Primary antibodies were as follows: rabbit poly-clonal anti-GR (#A2164, ABclonal), rabbit polyclonal anti-RNApol-II (A11181), mouse monoclonal ANTI-FLAG M2 (#F1804, Sigma-Aldrich, St. Louis, MO). Chromatin complexes were precipitated with 100 µl of Dynabeads M-280 (Sheep anti-mouse, # 11202D; sheep anti-rabbit, #11204; Thermo Fisher Scientific, Waltham, MA). After

washes and elution, samples were treated with proteinase K (Cat# 19131, QIAGEN, Hilden, Germany) at 55°C, and cross-linking was reversed through overnight incubation at 65°C. DNA was purified using a MinElute purification kit (Cat# 28004, QIAGEN, Hilden, Germany) and quantitated using Qubit reader and reagents. Library preparation and sequencing were conducted at the NU Genomics Core, using TruSeq ChIP-seq library prep (with size exclusion) on ~10 ng of chromatin per ChIP sample or pooled inputs and HiSeq 50-bp was conducted using HOMER software (v4.10) after aligning fastq files to the mm10 mouse genome using bowtie2. PCA was conducted using ClustVis. Heatmaps of peak density were imaged with TreeView3. Peak tracks were imaged through WashU epigenome browser. Gene ontology pathway enrichment was conducted using the gene ontology analysis tool.

2-DG-6-phosphatase assay

For measuring the uptake of 2-DG-6-phosphatase, Glucose uptake-Glo^{TM} assay (Cat# J1341, Promega) was utilized to inject 1mM 2DG into mice for 30 mins before euthanasia. After 30 mins, the whole heart tissues were harvested and stored at -80C until ready to use. Next, the reagents from the kit were combined for reaction mixtures according to manufacturer's instructions and incubated at room temperature for 1 hr. The frozen heart tissues were crushed into a fine powder and 20 - 50 mg of tissue powder was used for the assay. After 1 hour incubation of reaction mixture, 25 µl of Neutralization buffer was added to reaction mixture. Next, 125 µl of reaction mixture and neutralization buffer was added to powdered heart tissue and incubated for 1 hr. After incubation, the samples were centrifuged for 5 mins at 10,000*g* and 125 µl of the supernatant was loaded onto a 96-well plate for luminescence readings.

Respirometry on cardiomyocytes and isolated mitochondria

For cardiomyocytes, respiratory was performed on freshly isolated cells. Cardiomyocytes are isolated adapting to previously reported conditions. In anesthetized mice, the descending aorta is cut, and the heart is immediately flushed by injecting 7ml pre-warmed EDTA buffer into the right ventricle. Immediately afterwards, the ascending aorta is clamped using Reynolds forceps, the heart is removed and kept in the 60 mm dish with pre-warmed EDTA buffer. The digestion process is proceeded by injecting 10 ml pre-warmed EDTA buffer to the apex of left ventricle. The heart is then transferred to the 60 mm dish with perfusion buffer and 3 ml perfusion buffer is injected to flush out the EDTA buffer. Then the heart is transferred to another 60 mm dish with pre-warmed 180U/ml Collagenase II buffer and 30-40 ml collagenase buffer is injected into the apex of LV. Then the heart is cut from the clamp, the ventricular myocardial tissue is pulled gently into small pieces using forceps and further dissociated by gentle pipetting. The cardiomyocyte suspension is passed through a 200 µm mesh, and the digestion is stopped by adding 5ml of stop buffer. Cardiomyocytes are then centrifuged at 100*g* for 3 mins, resuspended in the stop buffer with increasing concentration of calcium (100 µM, 400 µM, and 1000 µM), re-centrifuged and then plated in laminin-coated Seahorse plates in culture media. After 1 h incubation, the culture media is aspirated and Seahorse media is added for respirometry, which starts after an additional 1 h equilibrium in a CO_2-free incubator. Buffer compositions: EDTA buffer contains 130 mM NaCl, 5mM KCl,

0.5mM NaH_2PO_4, 10mM HEPES, 10mM glucose, 10mM BDM, 10mM Taurine, 5 mM EDTA, pH 7.8; Perfusion buffer contains 130 mM NaCl, 5 mM KCl, 0.5 mM NaH_2PO_4, 10 mM HEPES, 10 mM glucose, 10 mM BDM, 10 mM taurine, 1 mM $MgCl_2$, pH 7.8; Collagenase buffer contains 220U/ml Collagenase II; Stop buffer consists of Perfusion buffer supplemented with 5% sterile fetal bovine serum; Culture medium (250 mL) contains 2.45g Hanks' salt, 5 mL non-essential amino acids, 2.5 mL MEM Vitamin Solution, 0.0875g $NaHCO_3$, 2.5 mL PenStrep 10X, 1 mg/mL bovine serum albumin. Regular seahorse protocol is followed with basal reads and injection of oligomycin, FCCP, Rotenone/Antimycin following reported conditions. Basal OCR was calculated as baseline value (average of 3 consecutive reads) minus value after rotenone/antimycin addition (average of 3 consecutive reads). Basal OCR values were normalized to total protein content, assayed in each well after the Seahorse ran through homogenization and Bradford assay. Mitochondrial ATP production rate was calculated as $OCR_{ATP} * 2$ (mol O in mol O_2) $*$ 2.75 (Seahorse P/O), where OCR_{ATP} is the difference between baseline and oligomycin OCR. Nutrients: 10 mM glucose or 10 mM pyruvate; inhibitors: 0.5 μM rotenone + 0.5 μM antimycin A (Agilent). Respiratory control ratio (RCR) values were obtained from isolated mitochondria from myocardial tissue. Tissues from the left ventricle are harvested from the mouse and cut up into very fine pieces. The minced tissue is placed in a 15 mL conical tube (USA Scientific #188261) and 5 mL of MS-EGTA buffer with 1 mg Trypsin (Sigma #T1426-50 MG) is added to the tube. The tube is quickly vortexed, and the tissue is left submerged in the solution. After 2 min, 5 mL of MS-EGTA buffer with 0.2% BSA (Goldbio #A-421-250) is added to the tube to stop the trypsin reaction. MS-EGTA buffer: Mannitol (#M0214-45, ChemProducts), Sucrose (#100892, Millipore), HEPES (#15630–080, Gibco), EGTA (#E14100–50.0, RPI). The tube is inverted several times to mix then set to rest. Once the tissue has settled to the bottom of the tube, 3 mL of buffer is aspirated, and the remaining solution and tissue is transferred to a 10 mL glass tissue homogenizer (Avantor # 89,026–382). Once sufficiently homogenized the solution is transferred back into the 15 mL conical tube and spun in the centrifuge at 1,000g for 5 min at 4 °C. After spinning, the supernatant is transferred to a new 15 mL conical tube. The supernatant in the new tube is then centrifuged at 12,000g for 10 min at 4 °C to pellet the mitochondria. The supernatant is discarded from the pellet and the pellet is then resuspended in 7 mL of MS-EGTA buffer and centrifuged again at 12,000g for 10 min at 4 °C. After spinning, the supernatant is discarded, and the mitochondria are resuspended in 1 mL of Seahorse medium (Agilent #103335–100) with supplemented 5 mM pyruvate (Sigma #P2256-100G). After protein quantitation using a Bradford assay (Bio-Rad #5000001), 2.5 μg mitochondria are dispensed per well in 180 μl total volumes and let to equilibrate for 1 h at 37 degrees C. 20 μl of 5 mM ADP (Sigma #01905), 50 μM Oligomycin (Milipore #495455-10 MG), 100 μM Carbonyl cyanide-p-trifluoromethoxyphenylhydrazone (TCI #C3463), and 5 μM Rotenone (Milipore #557368-1 GM)/Antimycin A (Sigma #A674-50 MG) are added to drug ports A, B, and C, respectively. At baseline and after each drug injection, samples are read three consecutive times. RCR was calculated as the ratio between state III (OCR after ADP addition) and uncoupled state IV (OCR after oligomycin addition). All Seahorse measurements were conducted blinded to treatment groups.

Western blotting

Protein analyses in liver were performed on ~ 50 ug total lysates from the whole heart. Cyro-pulverized liver tissue was incubated in RIPA buffer (Cat #89900, Thermo Fisher Scientific, Waltham, MA) supplemented with 1x protease/phosphatase inhibitor (Cat #78440, Thermo Fisher Scientific, Waltham, MA) for 30 mins and sonicated for 10 secs twice. The samples were then centrifuged at 10,000 rpm for 10 mins at 4°C. Supernatant containing the protein is transferred into a new tube and used as a total lysate. For total cell lysates from culture cells, cells were harvested and resuspended in RIPA buffer containing 1x protease and phosphatase inhibitors. Lysates were incubated for 30 mins and centrifuged at 10,000 rpm for 10 mins at 4°C. The supernatant was used as a total cell lysate. The protein concentrations of the supernatants were determined using the Pierce BCA Protein Assay kit (Cat #23227, Thermo Fisher Scientific, Waltham, MA). Equal amounts of protein were separated using SDS-PAGE and transferred to a PVDF membrane (Cat #1620174, BioRad, Hercules, CA). Membranes were blocked in 5% milk in TBST for 1 hour at room temperature and then incubated overnight at 4°C with primary antibodies: Rabbit *Klf15* polyclonal antibody (Cat# A7194, ABclonal), Rabbit *Gapdh* monoclonal antibody (Cat# A10868, ABclonal), followed by incubation with HRP-conjugated secondary antibodies: Peroxidase AffiniPure Goat Anti-Rabbit IgG (H+L) (Cat# 111-035-003, Jackson ImmunoResearch Labs, West Grove, PA) for 1 hour at room temperature. Immunoreactive bands were visualized by chemiluminescence using Pierce Enhanced Chemiluminescent western blotting substrate (Cat #32106, Thermo Fisher Scientific, Waltham, MA).

Echocardiography

Mice were anesthetized with 1.5% isoflurane (1.5% oxygen) and imaged in the supine position using Vevo 3100 Imaging System with a 35-MHz linear probe (Visualsonics, Canada). The core temperature was maintained at 37°C. Heart rates were kept consistent between the groups (400 – 450 bpm) [41]. The heart was imaged in a 2D, short axis, and 4-chamber view by placing the pulsed wave Doppler at the septal corner of the mitral annulus. Mitral inflow velocity (E) and longitudinal tissue velocity of the mitral anterior annulus (e') were measured through Vevo2100 1.5.0 Image Software [42].

Statistics

Statistical analyses were performed using Prism software v8.4.1 (Graphpad, La Jolla, CA). The Pearson-D'Agostino normality test was used to assess data distribution normality. When comparing two groups, two-tailed Student's t-test with Welch's correction (unequal variances) was used. When comparing three groups of data for one variable, one-way ANOVA with Sidak multi-comparison was used. When comparing data for more than one related variable, two-way ANOVA was used. For ANOVA and t-test analyses, a P value less than 0.05 was considered significant. When the number of data points was less than 10, data were presented as single values (dot plots, histograms). Analyses pooling data points over time were presented as line plots connecting medians of box plots showing distribution of all data per time point.

REFERENCES

[1] G. Jia, V.G. DeMarco, J.R. Sowers, Insulin resistance and hyperinsulinaemia in diabetic cardiomyopathy, Nat Rev Endocrinol 12(3) (2016) 144-53.

[2] Q.G. Karwi, Q. Sun, G.D. Lopaschuk, The Contribution of Cardiac Fatty Acid Oxidation to Diabetic Cardiomyopathy Severity, Cells 10(11) (2021).

[3] P.C. Schulze, K. Drosatos, I.J. Goldberg, Lipid Use and Misuse by the Heart, Circ Res 118(11) (2016) 1736-51.

[4] N.J. Morrish, S.L. Wang, L.K. Stevens, J.H. Fuller, H. Keen, Mortality and causes of death in the WHO Multinational Study of Vascular Disease in Diabetes, Diabetologia 44 Suppl 2 (2001) S14-21.

[5] R.M. de Guia, A.J. Rose, S. Herzig, Glucocorticoid hormones and energy homeostasis, Horm Mol Biol Clin Investig 19(2) (2014) 117-28.

[6] T. Seidel, D.J. Fiegle, T.J. Baur, A. Ritzer, S. Nay, C. Heim, M. Weyand, H. Milting, R.H. Oakley, J.A. Cidlowski, T. Volk, Glucocorticoids preserve the t-tubular system in ventricular cardiomyocytes by upregulation of autophagic flux, Basic Res Cardiol 114(6) (2019) 47.

[7] R.H. Oakley, R. Ren, D. Cruz-Topete, G.S. Bird, P.H. Myers, M.C. Boyle, M.D. Schneider, M.S. Willis, J.A. Cidlowski, Essential role of stress hormone signaling in cardiomyocytes for the prevention of heart disease, Proc Natl Acad Sci U S A 110(42) (2013) 17035-40.

[8] M. Pujades-Rodriguez, A.W. Morgan, R.M. Cubbon, J. Wu, Dose-dependent oral glucocorticoid cardiovascular risks in people with immune-mediated inflammatory diseases: A population-based cohort study, PLoS Med 17(12) (2020) e1003432.

[9] M. Quattrocelli, M. Wintzinger, K. Miz, M. Panta, A.D. Prabakaran, G.D. Barish, N.S. Chandel, E.M. McNally, Intermittent prednisone treatment in mice promotes exercise tolerance in obesity through adiponectin, J Exp Med 219(5) (2022).

[10] A.S. Zelikovich, B.C. Joslin, P. Casey, E.M. McNally, S. Ajroud-Driss, An Open Label Exploratory Clinical Trial Evaluating Safety and Tolerability of Once-Weekly Prednisone in Becker and Limb-Girdle Muscular Dystrophy, J Neuromuscul Dis 9(2) (2022) 275-287.

[11] M. Wintzinger, M. Panta, K. Miz, A.D. Prabakaran, H.B. Durumutla, M. Sargent, C.B. Peek, J. Bass, J.D. Molkentin, M. Quattrocelli, Impact of circadian time of dosing on cardiomyocyte-autonomous effects of glucocorticoids, Mol Metab 62 (2022) 101528.

[12] S.K. Sasse, Z. Zuo, V. Kadiyala, L. Zhang, M.A. Pufall, M.K. Jain, T.L. Phang, G.D. Stormo, A.N. Gerber, Response Element Composition Governs Correlations between Binding Site Affinity and Transcription in Glucocorticoid Receptor Feed-forward Loops, J Biol Chem 290(32) (2015) 19756-69.

[13] D.A. Prosdocimo, J.E. John, L. Zhang, E.S. Efraim, R. Zhang, X. Liao, M.K. Jain, KLF15 and PPARalpha Cooperate to Regulate Cardiomyocyte Lipid Gene Expression and Oxidation, PPAR Res 2015 (2015) 201625.

[14] L. Fan, P.N. Hsieh, D.R. Sweet, M.K. Jain, Kruppel-like factor 15: Regulator of BCAA metabolism and circadian protein rhythmicity, Pharmacol Res 130 (2018) 123-126.

[15] A.Y. So, T.U. Bernal, M.L. Pillsbury, K.R. Yamamoto, B.J. Feldman, Glucocorticoid regulation of the circadian clock modulates glucose homeostasis, Proc Natl Acad Sci U S A 106(41) (2009) 17582-7.

[16] H. Oster, S. Damerow, S. Kiessling, V. Jakubcakova, D. Abraham, J. Tian, M.W. Hoffmann, G. Eichele, The circadian rhythm of glucocorticoids is regulated by a gating mechanism residing in the adrenal cortical clock, Cell Metab 4(2) (2006) 163-73.

[17] K.A. Lamia, S.J. Papp, R.T. Yu, G.D. Barish, N.H. Uhlenhaut, J.W. Jonker, M. Downes, R.M. Evans, Cryptochromes mediate rhythmic repression of the glucocorticoid receptor, Nature 480(7378) (2011) 552-6.

[18] L. Rizzini, D.C. Levine, M. Perelis, J. Bass, C.B. Peek, M. Pagano, Cryptochromes-Mediated Inhibition of the CRL4(Cop1)-Complex Assembly Defines an Evolutionary Conserved Signaling Mechanism, Curr Biol 29(12) (2019) 1954-1962 e4.

[19] S. Gong, Y.L. Miao, G.Z. Jiao, M.J. Sun, H. Li, J. Lin, M.J. Luo, J.H. Tan, Dynamics and correlation of serum cortisol and corticosterone under different physiological or stressful conditions in mice, PloS one 10(2) (2015) e0117503.

[20] N. Nader, G.P. Chrousos, T. Kino, Circadian rhythm transcription factor CLOCK regulates the transcriptional activity of the glucocorticoid receptor by acetylating its hinge region lysine cluster: potential physiological implications, FASEB J 23(5) (2009) 1572-83.

[21] L. Zhang, D.A. Prosdocimo, X. Bai, C. Fu, R. Zhang, F. Campbell, X. Liao, J. Coller, M.K. Jain, KLF15 Establishes the Landscape of Diurnal Expression in the Heart, Cell Rep 13(11) (2015) 2368-2375.

[22] W.L. Holland, J.Y. Xia, J.A. Johnson, K. Sun, M.J. Pearson, A.X. Sharma, E. Quittner-Strom, T.S. Tippetts, R. Gordillo, P.E. Scherer, Inducible overexpression of adiponectin receptors highlight the roles of adiponectin-induced ceramidase signaling in lipid and glucose homeostasis, Mol Metab 6(3) (2017) 267-275.
[23] S. Keshvari, D.C. Henstridge, C. Ng, M.A. Febbraio, J.P. Whitehead, Muscle-specific overexpression of AdipoR1 or AdipoR2 gives rise to common and discrete local effects whilst AdipoR2 promotes additional systemic effects, Sci Rep 7 (2017) 41792.
[24] M. Fernandez-Caggiano, A. Kamynina, A.A. Francois, O. Prysyazhna, T.R. Eykyn, S. Krasemann, M.G. Crespo-Leiro, M.G. Vieites, K. Bianchi, V. Morales, N. Domenech, P. Eaton, Mitochondrial pyruvate carrier abundance mediates pathological cardiac hypertrophy, Nat Metab 2(11) (2020) 1223-1231.
[25] Y. Zhang, P.V. Taufalele, J.D. Cochran, I. Robillard-Frayne, J.M. Marx, J. Soto, A.J. Rauckhorst, F. Tayyari, A.D. Pewa, L.R. Gray, L.M. Teesch, P. Puchalska, T.R. Funari, R. McGlauflin, K. Zimmerman, W.J. Kutschke, T. Cassier, S. Hitchcock, K. Lin, K.M. Kato, J.L. Stueve, L. Haff, R.M. Weiss, J.E. Cox, J. Rutter, E.B. Taylor, P.A. Crawford, E.D. Lewandowski, C. Des Rosiers, E.D. Abel, Mitochondrial pyruvate carriers are required for myocardial stress adaptation, Nat Metab 2(11) (2020) 1248-1264.
[26] A.A. Cluntun, R. Badolia, S. Lettlova, K.M. Parnell, T.S. Shankar, N.A. Diakos, K.A. Olson, I. Taleb, S.M. Tatum, J.A. Berg, C.N. Cunningham, T. Van Ry, A.J. Bott, A.T. Krokidi, S. Fogarty, S. Skedros, W.I. Swiatek, X. Yu, B. Luo, S. Merx, S. Navankasattusas, J.E. Cox, G.S. Ducker, W.L. Holland, S.H. McKellar, J. Rutter, S.G. Drakos, The pyruvate-lactate axis modulates cardiac hypertrophy and heart failure, Cell Metab 33(3) (2021) 629-648 e10.
[27] S.M. Haldar, Y. Lu, D. Jeyaraj, D. Kawanami, Y. Cui, S.J. Eapen, C. Hao, Y. Li, Y.Q. Doughman, M. Watanabe, K. Shimizu, H. Kuivaniemi, J. Sadoshima, K.B. Margulies, T.P. Cappola, M.K. Jain, Klf15 deficiency is a molecular link between heart failure and aortic aneurysm formation, Sci Transl Med 2(26) (2010) 26ra26.
[28] D.A. Prosdocimo, P. Anand, X. Liao, H. Zhu, S. Shelkay, P. Artero-Calderon, L. Zhang, J. Kirsh, D. Moore, M.G. Rosca, E. Vazquez, J. Kerner, K.M. Akat, Z. Williams, J. Zhao, H. Fujioka, T. Tuschl, X. Bai, P.C. Schulze, C.L. Hoppel, M.K. Jain, S.M. Haldar, Kruppel-like factor 15 is a critical regulator of cardiac lipid metabolism, J Biol Chem 289(9) (2014) 5914-24.
[29] S. Sakamuri, J.A. Sperling, V.N. Sure, M.H. Dholakia, N.R. Peterson, I. Rutkai, P.S. Mahalingam, R. Satou, P.V.G. Katakam, Measurement of respiratory function in isolated cardiac mitochondria using Seahorse XFe24 Analyzer: applications for aging research, Geroscience 40(3) (2018) 347-356.
[30] M. Quattrocelli, M. Wintzinger, K. Miz, D.C. Levine, C.B. Peek, J. Bass, E.M. McNally, Muscle mitochondrial remodeling by intermittent glucocorticoid drugs requires an intact circadian clock and muscle PGC1alpha, Sci Adv 8(7) (2022) eabm1189.
[31] Z. Jiang, S.Z. Elsarrag, Q. Duan, E.L. LaGory, Z. Wang, M. Alexanian, S. McMahon, I.C. Rulifson, S. Winchester, Y. Wang, C. Vaisse, J.D. Brown, M. Quattrocelli, C.Y. Lin, S.M. Haldar, KLF15 cistromes reveal a hepatocyte pathway governing plasma corticosteroid transport and systemic inflammation, Sci Adv 8(10) (2022) eabj2917.
[32] J. Mori, V.B. Patel, O. Abo Alrob, R. Basu, T. Altamimi, J. Desaulniers, C.S. Wagg, Z. Kassiri, G.D. Lopaschuk, G.Y. Oudit, Angiotensin 1-7 ameliorates diabetic cardiomyopathy and diastolic dysfunction in db/db mice by reducing lipotoxicity and inflammation, Circ Heart Fail 7(2) (2014) 327-39.
[33] L. Alex, I. Russo, V. Holoborodko, N.G. Frangogiannis, Characterization of a mouse model of obesity-related fibrotic cardiomyopathy that recapitulates features of human heart failure with preserved ejection fraction, Am J Physiol Heart Circ Physiol 315(4) (2018) H934-H949.
[34] W.L. Holland, R.A. Miller, Z.V. Wang, K. Sun, B.M. Barth, H.H. Bui, K.E. Davis, B.T. Bikman, N. Halberg, J.M. Rutkowski, M.R. Wade, V.M. Tenorio, M.S. Kuo, J.T. Brozinick, B.B. Zhang, M.J. Birnbaum, S.A. Summers, P.E. Scherer, Receptor-mediated activation of ceramidase activity initiates the pleiotropic actions of adiponectin, Nat Med 17(1) (2011) 55-63.
[35] B.C. Field, R. Gordillo, P.E. Scherer, The Role of Ceramides in Diabetes and Cardiovascular Disease Regulation of Ceramides by Adipokines, Front Endocrinol (Lausanne) 11 (2020) 569250.
[36] D. Yazici, H. Sezer, Insulin Resistance, Obesity and Lipotoxicity, Adv Exp Med Biol 960 (2017) 277-304.
[37] A.R. Wende, J.C. Schell, C.M. Ha, M.E. Pepin, O. Khalimonchuk, H. Schwertz, R.O. Pereira, M.K. Brahma, J. Tuinei, A. Contreras-Ferrat, L. Wang, C.A. Andrizzi, C.D. Olsen, W.E. Bradley, L.J. Dell'Italia, W.H. Dillmann, S.E. Litwin, E.D. Abel, Maintaining Myocardial Glucose Utilization in Diabetic Cardiomyopathy Accelerates Mitochondrial Dysfunction, Diabetes 69(10) (2020) 2094-2111.
[38] K.S. McCommis, A. Kovacs, C.J. Weinheimer, T.M. Shew, T.R. Koves, O.R. Ilkayeva, D.R. Kamm, K.D. Pyles, M.T. King, R.L. Veech, B.J. DeBosch, D.M. Muoio, R.W. Gross, B.N. Finck, Nutritional modulation of heart failure in mitochondrial pyruvate carrier-deficient mice, Nat Metab 2(11) (2020) 1232-1247.

[39] S.S. Vadvalkar, S. Matsuzaki, C.A. Eyster, J.R. Giorgione, L.B. Bockus, C.S. Kinter, M. Kinter, K.M. Humphries, Decreased Mitochondrial Pyruvate Transport Activity in the Diabetic Heart: ROLE OF MITOCHONDRIAL PYRUVATE CARRIER 2 (MPC2) ACETYLATION, J Biol Chem 292(11) (2017) 4423-4433.
[40] M. Saito, G.A. Bray, Diurnal rhythm for corticosterone in obese (ob/ob) diabetes (db/db) and gold-thioglucose-induced obesity in mice, Endocrinology 113(6) (1983) 2181-5.
[41] M. Schnelle, N. Catibog, M. Zhang, A.A. Nabeebaccus, G. Anderson, D.A. Richards, G. Sawyer, X. Zhang, K. Toischer, G. Hasenfuss, M.J. Monaghan, A.M. Shah, Echocardiographic evaluation of diastolic function in mouse models of heart disease, J Mol Cell Cardiol 114 (2018) 20-28.
[42] E.M. Jeong, J. Chung, H. Liu, Y. Go, S. Gladstein, A. Farzaneh-Far, E.D. Lewandowski, S.C. Dudley, Jr., Role of Mitochondrial Oxidative Stress in Glucose Tolerance, Insulin Resistance, and Cardiac Diastolic Dysfunction, J Am Heart Assoc 5(5) (2016).